

Equation of state of superfluid neutron matter with low-momentum interactions

Viswanathan Palaniappan,^{1,2,*} S. Ramanan,^{1,†} and Michael Urban^{2,‡}

¹*Department of Physics, Indian Institute of Technology Madras, Chennai - 600036, India*

²*Université Paris-Saclay, CNRS-IN2P3, IJCLab, 91405 Orsay, France*

In this work, we calculate the ground state energy of pure neutron matter using the renormalization group based low-momentum effective interaction $V_{\text{low-}k}$ in Bogoliubov many-body perturbation theory (BMBPT), which is a perturbative expansion around the Hartree-Fock-Bogoliubov (HFB) ground state. In order to capture the low-density behavior of neutron matter, it turns out to be better to use a density dependent cutoff in the $V_{\text{low-}k}$ interaction. Perturbative corrections to the HFB energy up to third order are included. We find that at low densities corresponding to the inner crust of neutron stars, the HFB state that includes pairing is a better starting point for perturbation expansion. It is observed that including the higher order perturbative corrections, the cutoff dependence of the ground state energy is reduced.

I. INTRODUCTION

Neutron stars consist of several layers called the outer crust, inner crust, outer core, and inner core. The outer crust is made of nuclei that get progressively neutron rich, and a degenerate electron gas to ensure charge neutrality [1]. At some point, the neutrons can no longer be bound, forming a gas of neutrons interspersing a lattice of quasi-nuclei (clusters). This defines the inner crust. The outer core consists of very neutron rich uniform nuclear matter, while the composition of the inner core remains an open question. While the crust itself extends just over 2 km, understanding its structure is crucial to explain certain observations. The unbound neutrons in the inner crust are believed to be in a superfluid phase, which is necessary to explain the observed pulsar glitches [2]. (However, for a detailed understanding of the pulsar glitches, one has to take into account the effect of the entrainment of the superfluid neutrons by the lattice of clusters [3–5] as well as the pinning of superfluid vortices [6].) Furthermore, neutron pairing plays an important role in the thermal evolution of the star [7]. While superfluidity in neutron-star crusts was predicted as early as 1960 [8], a quantitatively reliable theoretical description still eludes the community, largely due to the uncertainties in the input two-body interaction and the subsequent medium and higher-body corrections.

Pure neutron matter is a simple yet useful model for a neutron star. In first approximation, it describes the gas of unbound neutrons in the inner crust, neglecting the presence of the clusters. Furthermore, the properties of the inner crust including the clusters depend sensitively on the equation of state of the neutron gas, because the inner crust can be regarded as a phase coexistence of a liquid and a gas phase [9]. At low densities, corresponding to the inner crust, the neutron-neutron (nn) interaction is attractive in the 1S_0 partial wave, resulting

in the formation of spin-singlet Cooper pairs. At higher densities, i.e. in the outer layers of the core, pairing occurs between neutrons in the spin-triplet ($^3P_2 - ^3F_2$) channel. At the BCS level (i.e., free-space nn interaction and single-particle spectrum), 1S_0 pairing is completely constrained by two-body scattering in free space. However, corrections beyond BCS are important, and the gap equation is very sensitive to such corrections. For example, it was seen in [10] that already the inclusion of the effective mass from different effective interactions in the single-particle energies introduces model dependence in the 1S_0 gaps. On the other hand, at the high densities as they are found in the outer core, the triplet channel gaps are highly model dependent [11–15] and it is not surprising that a proper description of triplet pairing requires the inclusion of the three-nucleon force at the very least (see for example [12–15]).

Because of the fact that the nn scattering length $a \approx -18$ fm is much larger than the effective range $r_e \approx 2.7$ fm of the nn interaction, it was suggested by Bertsch that dilute neutron matter could be in a first approximation modeled as a unitary Fermi gas (defined by $a \rightarrow \infty$ and $r_e \rightarrow 0$) [16]. In the meanwhile, the experimental realization of the unitary Fermi gas and of the BCS-BEC crossover with ultracold trapped atoms has boosted also a lot of theoretical activity in this field, see [17] for a review. The present work extends our previous study for ultracold Fermi gases [18] to pure neutron matter. While ultracold atoms have tunable scattering length a (via Feshbach resonance) and negligible effective range r_e , both these quantities are fixed in pure neutron matter by the nn interaction. Only as long as the effects of the effective range can be neglected, both these systems exhibit universal behavior. In [18], we studied the equation of state of a gas of ultracold fermions from the BCS regime ($1/k_F a \rightarrow -\infty$, where k_F is the Fermi momentum) to the unitary limit ($1/k_F a \rightarrow 0$), starting with the Hartree-Fock-Bogoliubov (HFB) energy, computed with a $V_{\text{low-}k}$ like interaction tailored for the cold atomic systems, and then including corrections to the HFB energy up to third order within the Bogoliubov many-body perturbation theory (BMBPT). In addition, we used the de-

* viswanathan@physics.iitm.ac.in

† suna@physics.iitm.ac.in

‡ michael.urban@ijclab.in2p3.fr

pendence of the results on the cutoff of the effective low-momentum interaction to gain additional insights on the convergence of this scheme.

The main focus of our current work is to adapt a strategy that was successfully used in nuclear structure calculations of finite nuclei [19], to the case of infinite neutron matter. The aim is to obtain reliable results for the neutron-matter equation of state starting from a realistic nn interaction, by performing essentially three steps: (1) The initial interaction is softened using renormalization-group (RG) techniques, lowering the momentum cutoff Λ while keeping low-energy two-body observables unchanged [20–23]. (2) The resulting $V_{\text{low-}k}$ interaction is used in HFB approximation. (3) Corrections beyond HFB are included using BMBPT. In contrast to studies of finite nuclei, since we are considering uniform matter, we can use a density dependent cutoff $\Lambda = fk_F$, where f is a scale factor. Such a scaling was used for the first time in [24]. Previous studies [18, 25] have demonstrated that a variable cutoff is especially important to describe the low-density limit. Since Λ is an unphysical parameter, any dependence of the equation of state on Λ or on the scale factor f gives an indication for the importance of missing three-body and medium corrections.

Our study is similar in spirit to the work by Coraggio et al. [26], who compared results obtained with interactions having different regulator functions, using the Hartree-Fock (HF) instead of the HFB approximation as a starting point and third-order many-body perturbation theory (MBPT). They showed that the dependence on the choice of the regulator is to a large extent compensated if in addition to the two-body also three-body interactions are included. However, that work focused on higher densities where pairing effects on the equation of state are weak, and where the use of a density dependent cutoff is not required. If one is interested in superfluidity, it is of course mandatory to start from the HFB and not from the HF ground state.

The paper is organized as follows. Sect. II discusses the BMBPT formalism and obtains expressions for the second and third order corrections to the HFB energy. The main results are discussed in Sect. III, while in Sect. IV, we summarize the important aspects of our current work and look at possible directions that could be explored in future studies.

II. FORMALISM

In this section, we outline the BMBPT, by first reviewing the HFB approach to incorporate the superfluid nature of the ground state.

A. Hartree-Fock-Bogoliubov Theory

The pairing between two particles in the states $\mathbf{k} \uparrow$ and $-\mathbf{k} \downarrow$ in an interacting Fermi gas can be realized via the

definition of a new quasiparticle operator [27]

$$\beta_{\mathbf{k}\sigma} = u_k a_{\mathbf{k}\sigma} - (-1)^{\frac{1}{2}-\sigma} v_k a_{-\mathbf{k}-\sigma}^\dagger, \quad (1)$$

where the coefficients u_k and v_k can be chosen to be real, $a_{\mathbf{k}\sigma}$ and $a_{\mathbf{k}\sigma}^\dagger$ are particle annihilation and creation operators, and $\sigma = \pm\frac{1}{2}$ labels the spin projection. For the transformation to be canonical, the quasiparticle operators have to satisfy the usual anticommutation relations and as a result, the coefficients are constrained to obey the condition $u_k^2 + v_k^2 = 1$. Since the particle number is not conserved in this approach, one fixes the average particle number (or number density n) by introducing the chemical potential μ and writing the grand canonical Hamiltonian as

$$\begin{aligned} \hat{K} = & \hat{H} - \mu \hat{N} \\ = & \sum_{\mathbf{k}\sigma} (\varepsilon_k^0 - \mu) a_{\mathbf{k}\sigma}^\dagger a_{\mathbf{k}\sigma} \\ & + \frac{1}{4} \sum_{\mathbf{k}_i \sigma_i} \langle \mathbf{k}_1 \sigma_1 \mathbf{k}_2 \sigma_2 | \bar{V} | \mathbf{k}_3 \sigma_3 \mathbf{k}_4 \sigma_4 \rangle \\ & \times a_{\mathbf{k}_1 \sigma_1}^\dagger a_{\mathbf{k}_2 \sigma_2}^\dagger a_{\mathbf{k}_4 \sigma_4} a_{\mathbf{k}_3 \sigma_3}. \end{aligned} \quad (2)$$

The second sum is over all momenta (with the constraint of momentum conservation) and spins. Since we are considering infinite matter, the sums over momenta will actually be integrals as in Ref. [18]. Further, $\varepsilon_k^0 = k^2/2m$ denotes the energy of a free neutron with mass m , \hat{N} is the particle-number operator, and \bar{V} is the antisymmetrized potential whose matrix elements are given in terms of those in the partial wave basis by

$$\begin{aligned} \langle \mathbf{k}_1 \sigma_1 \mathbf{k}_2 \sigma_2 | \bar{V} | \mathbf{k}_3 \sigma_3 \mathbf{k}_4 \sigma_4 \rangle = & (4\pi)^2 \sum_{sm_s m'_s} \sum_{ll' m_l m'_l} \sum_{jm_j} C_{\frac{1}{2}\sigma_1 \frac{1}{2}\sigma_2}^{sm_s} C_{\frac{1}{2}\sigma_3 \frac{1}{2}\sigma_4}^{sm'_s} \\ & \times C_{lm_l sm_s}^{jm_j} C_{l'm'_l sm'_s}^{jm'_j} Y_{lm_l}(\hat{\mathbf{q}}_{12}) Y_{l'm'_l}^*(\hat{\mathbf{q}}_{34}) \\ & \times i^{l-l'} V_{jll's}(q_{12}, q_{34}) [1 + (-1)^{l+s}]. \end{aligned} \quad (3)$$

where $\mathbf{q}_{ij} = (\mathbf{k}_i - \mathbf{k}_j)/2$, $C_{j_1 m_1 j_2 m_2}^{jm}$ are the Clebsch-Gordan coefficients in the notation of Ref. [28] and Y_{lm} the spherical harmonics. Rewriting the expression for the Hamiltonian in terms of the quasiparticle operators, Eq. (2) becomes

$$\begin{aligned} \hat{K} = & \sum_{\mathbf{k}} [2v_k^2 \xi_k - v_k^2 \Sigma_{\text{HFB}}(k) - u_k v_k \Delta_k] \\ & + \sum_{\mathbf{k}, \sigma} \beta_{\mathbf{k}\sigma}^\dagger \beta_{\mathbf{k}\sigma} [(u_k^2 - v_k^2) \xi_k + 2u_k v_k \Delta_k] \\ & + \frac{1}{2} \sum_{\mathbf{k}, \sigma} (-1)^{\frac{1}{2}-\sigma} [\beta_{-\mathbf{k}-\sigma} \beta_{\mathbf{k}\sigma} + \beta_{\mathbf{k}\sigma}^\dagger \beta_{-\mathbf{k}-\sigma}^\dagger] \\ & \times [2u_k v_k \xi_k - (u_k^2 - v_k^2) \Delta_k] + \mathcal{N}(\hat{V}), \end{aligned} \quad (4)$$

where $\Sigma_{\text{HFB}}(k)$ and Δ_k are, respectively, the HFB self-energy and the 1S_0 gap function whose expressions will

be given below and ξ_k denotes the single-particle energy measured with respect to the chemical potential,

$$\xi_k \equiv \varepsilon_k^0 + \Sigma_{\text{HFB}}(k) - \mu. \quad (5)$$

The symbol \mathcal{N} in Eq. (4) denotes normal ordering with respect to the quasiparticle operators (moving β^\dagger operators to the left and β operators to the right), and $\mathcal{N}(\hat{V})$ is given by

$$\begin{aligned} \mathcal{N}(\hat{V}) = & \frac{1}{4} \sum_{\mathbf{k}_i \sigma_i} \langle \mathbf{k}_1 \sigma_1 \mathbf{k}_2 \sigma_2 | \bar{V} | \mathbf{k}_3 \sigma_3 \mathbf{k}_4 \sigma_4 \rangle \\ & \times \mathcal{N}(a_{\mathbf{k}_1 \sigma_1}^\dagger a_{\mathbf{k}_2 \sigma_2}^\dagger a_{\mathbf{k}_4 \sigma_4} a_{\mathbf{k}_3 \sigma_3}). \end{aligned} \quad (6)$$

As usual, one requires the third term in Eq. (4) to vanish, which leads to

$$u_k v_k = \frac{\Delta_k}{2E_k}, \quad u_k^2 = \frac{1}{2} \left(1 + \frac{\xi_k}{E_k} \right), \quad v_k^2 = \frac{1}{2} \left(1 - \frac{\xi_k}{E_k} \right), \quad (7)$$

where

$$E_k \equiv \sqrt{\Delta_k^2 + \xi_k^2} \quad (8)$$

is the quasiparticle energy. The 1S_0 gap and HFB self-energy are given by

$$\Delta_k = -\frac{1}{\pi} \int dk' k'^2 \frac{\Delta_{k'}}{E_{k'}} V_{^1S_0}(k, k'), \quad (9)$$

$$\Sigma_{\text{HFB}}(k) = \frac{1}{\pi} \int dk' k'^2 v_{k'}^2 \bar{V}_{\text{avg}}(k, k'). \quad (10)$$

In Eq. (10), $\bar{V}_{\text{avg}}(k, k')$ denotes the angle averaged interaction

$$\begin{aligned} \bar{V}_{\text{avg}}(k, k') = & \frac{1}{2} \int d(\cos \theta_{\mathbf{k}', \mathbf{k}}) \sum_{slj} (2j+1) \\ & \times V_{sllj}(q, q) [1 + (-1)^{l+s}], \end{aligned} \quad (11)$$

where $\mathbf{q} = (\mathbf{k} - \mathbf{k}')/2$. In the limit of zero gap, the factor v_k^2 becomes the Heaviside θ function and Eq. (10) reduces to the familiar HF self-energy. For a given chemical potential, the number density in the HFB approximation is given by

$$n_{\text{HFB}} = \frac{1}{\pi^2} \int dk k^2 v_k^2, \quad (12)$$

and the HFB ground state energy density is given by

$$\mathcal{E}_{\text{HFB}} = \frac{1}{2\pi^2} \int dk k^2 \left[v_k^2 (k^2 + \Sigma_{\text{HFB}}(k)) - \frac{\Delta_k^2}{E_k} \right]. \quad (13)$$

The energy per particle E_{HFB} is $\mathcal{E}_{\text{HFB}}/n_{\text{HFB}}$.

B. Bogoliubov Many-Body Perturbation Theory

With Eq. (7), the operator \hat{K} of Eq. (4) can now be rewritten as

$$\hat{K} = K_{00} + \hat{K}_{11} + \mathcal{N}(\hat{V}), \quad (14)$$

where \hat{K}_{ij} contains i quasiparticle creation operators and j quasiparticle annihilation operators. For example, K_{00} and \hat{K}_{11} are given by

$$K_{00} = \sum_{\mathbf{k}} \left(v_k^2 [2\xi_k - \Sigma_{\text{HFB}}(k)] - \frac{\Delta_k^2}{2E_k} \right), \quad (15)$$

$$\hat{K}_{11} = \sum_{\mathbf{k}, \sigma} \beta_{\mathbf{k} \sigma}^\dagger \beta_{\mathbf{k} \sigma} E_k, \quad (16)$$

where K_{00} corresponds to the expectation value of the operator \hat{K} in the HFB ground state which has zero quasiparticles, and \hat{K}_{11} describes the energy of non-interacting quasiparticles. The interaction between quasiparticles is contained in $\mathcal{N}(\hat{V})$, which can be written as

$$\mathcal{N}(\hat{V}) = \hat{K}_{40} + \hat{K}_{31} + \hat{K}_{22} + \hat{K}_{13} + \hat{K}_{04}. \quad (17)$$

Since the eigenstates and eigenvalues of $\hat{K}_0 = K_{00} + \hat{K}_{11}$ are known, one can build corrections to the HFB ground state through perturbation theory, i.e., by writing

$$\hat{K} = \hat{K}_0 + \lambda \mathcal{N}(\hat{V}) \quad (18)$$

and expanding the ground state of \hat{K} in powers of the formal parameter λ , the physical situation corresponding of course to $\lambda = 1$. Following [18, 19], there is no first-order correction and the second-order (BMBPT2) correction to the ground-state energy density¹ is given by

$$\mathcal{E}^{(2)} = -\frac{1}{4!} \sum_{1234} \frac{|\langle 0 | \hat{K}_{04} | 1234 \rangle|^2}{E_{1234}}, \quad (19)$$

where $|0\rangle$ is the HFB ground state, the indices 1, 2, 3, and 4 mean both momentum and spin, e.g., $1 = \{\mathbf{k}_1, \sigma_1\}$, such that the summation over 1234 means summation over momenta $\mathbf{k}_1 \dots \mathbf{k}_4$ (with zero total momentum $\mathbf{k}_1 + \mathbf{k}_2 + \mathbf{k}_3 + \mathbf{k}_4 = 0$) and spins $\sigma_1 \dots \sigma_4$. The energy of the intermediate four-quasiparticle state $|1234\rangle = \beta_1^\dagger \beta_2^\dagger \beta_3^\dagger \beta_4^\dagger |0\rangle$ is given by $E_{1234} = E_{k_1} + E_{k_2} + E_{k_3} + E_{k_4}$. The factor $4!$ accounts for the number of permutations of indices 1234 describing all the same state. The explicit form of the operator \hat{K}_{04} in Eq. (19) is

$$\begin{aligned} \hat{K}_{04} = & -\frac{1}{4} \sum_{1234} \langle 1 2 | \bar{V} | 3 4 \rangle (-1)^{\sigma_1 + \sigma_2} \\ & \times v_1 v_2 u_4 u_3 \beta_{-1} \beta_{-2} \beta_4 \beta_3. \end{aligned} \quad (20)$$

¹ As mentioned in Ref. [18], for a given chemical potential μ , the second- and third-order corrections to the grand potential $\Omega = \mathcal{E} - \mu n$ coincide with the second- and third-order corrections to the energy density of the system with the density $n_{\text{HFB}}(\mu)$.

where $v_1 = v_{k_1}$, etc. With a bit of algebra, it can be shown that the second-order correction to the energy is given by

$$\mathcal{E}^{(2)} = - \sum_{\mathbf{k}_1 \mathbf{k}_2 \mathbf{k}_3} \frac{A + B + C}{E_{1234}}, \quad (21)$$

where

$$A = \frac{1}{4} v_1^2 v_2^2 u_3^2 u_4^2 \sum_{\sigma_1 \sigma_2 \sigma_3 \sigma_4} |\langle -1 - 2 | \bar{V} | 3 4 \rangle|^2, \quad (22)$$

$$B = \frac{1}{4} u_1 v_2 u_2 v_2 u_3 v_3 u_4 v_4 \sum_{\sigma_1 \sigma_2 \sigma_3 \sigma_4} |\langle -1 - 2 | \bar{V} | 3 4 \rangle|^2, \quad (23)$$

$$C = v_1^2 u_2 v_2 u_3 v_3 u_4^2 \sum_{\sigma_1 \sigma_2 \sigma_3 \sigma_4} (-1)^{\sigma_2 + \sigma_3} \times \text{Re} \left[\langle -1 - 2 | \bar{V} | 3 4 \rangle^* \langle -1 - 3 | \bar{V} | 2 4 \rangle \right]. \quad (24)$$

The terms B and C contribute only when there is a finite gap. In the limit of no pairing, only term A contributes, and one retrieves the HF+MBPT2 as already noted in [18]. In deriving Eqs. (22)-(24), the hermiticity

$$\langle 1 2 | \bar{V} | 3 4 \rangle = \langle 3 4 | \bar{V} | 1 2 \rangle^*, \quad (25)$$

and the time-reversal symmetry

$$\langle 1 2 | \bar{V} | 3 4 \rangle = (-1)^{\sigma_1 + \sigma_2 + \sigma_3 + \sigma_4} \langle -3 - 4 | \bar{V} | -1 - 2 \rangle, \quad (26)$$

have been used.

Similarly, the third-order (BMBPT3) correction to the ground state energy density is given by

$$\mathcal{E}^{(3)} = \sum_{1 \dots 8} \frac{\langle 0 | \hat{K}_{04} | 1234 \rangle \langle 1234 | \hat{K}_{22} | 5678 \rangle \langle 5678 | \hat{K}_{40} | 0 \rangle}{E_{1234} E_{5678}}, \quad (27)$$

where $\hat{K}_{40} = \hat{K}_{04}^\dagger$ and

$$\begin{aligned} \hat{K}_{22} = & \frac{1}{4} \sum_{1234} \langle 1 2 | \bar{V} | 3 4 \rangle [u_1 u_2 u_4 u_3 \beta_1^\dagger \beta_2^\dagger \beta_4 \beta_3 \\ & + (-1)^{\sigma_1 + \sigma_2 + \sigma_3 + \sigma_4} v_1 v_2 v_4 v_3 \beta_{-4}^\dagger \beta_{-3}^\dagger \beta_{-1} \beta_{-2} \\ & - (-1)^{\sigma_2 + \sigma_3} u_1 v_2 u_4 v_3 \beta_1^\dagger \beta_{-3}^\dagger \beta_{-2} \beta_4 \\ & + (-1)^{\sigma_2 + \sigma_4} u_1 v_2 v_4 u_3 \beta_1^\dagger \beta_{-4}^\dagger \beta_{-2} \beta_3 \\ & + (-1)^{\sigma_1 + \sigma_3} v_1 u_2 u_4 v_3 \beta_2^\dagger \beta_{-3}^\dagger \beta_{-1} \beta_4 \\ & - (-1)^{\sigma_1 + \sigma_4} v_1 u_2 v_4 u_3 \beta_2^\dagger \beta_{-4}^\dagger \beta_{-1} \beta_3]. \end{aligned} \quad (28)$$

For ease of presentation, the lengthy explicit expressions at third order (that were obtained with the help of a Mathematica code) are relegated to the appendix. Momentum conservation finally reduces the number of momentum integrations to four.

The momentum integrals are computed numerically using Monte-Carlo integration with the importance-sampling method explained in Ref. [18].

III. RESULTS AND DISCUSSION

A. HFB results

Before we present our results, let us say a few words about the interaction used in our computations. We use the free-space RG-based low-momentum interaction $V_{\text{low-}k}$ (with a smooth exponential regulator with $n_{\text{exp}} = 5$), which depends on the renormalization cutoff Λ [22]. Lowering the cutoff through the RG flow softens the interaction while preserving two-body observables by construction. Furthermore, for cutoffs below $\Lambda \lesssim 2.1 \text{ fm}^{-1}$, the $V_{\text{low-}k}$ matrix elements become practically independent of the choice of the initial interaction such as AV18 or chiral potentials [23]. Here we will show results obtained with the $V_{\text{low-}k}$ derived from AV18 [29], but when starting from the N3LO chiral interaction [30] we obtain very similar results.

When such soft interactions are used in a many-body calculation, one hopes that perturbative corrections show rapid convergence. The two-body interaction eventually flows to the two-body scattering length as $\Lambda \rightarrow 0$. Therefore, small cutoffs become very important for describing physics at low densities (which otherwise would require ladder resummations), as was observed in [25]. There, a density dependent cutoff $\Lambda = f k_F$, with a scale factor f of the order of 2.5 (sufficiently large to leave the BCS gap unchanged), was required to reproduce the Gor'kov-Melik-Barkhudarov results for the superfluid transition temperature when screening effects are included. In a subsequent study [18], a $V_{\text{low-}k}$ like interaction was used to describe Fermi gases with contact interactions, and at least for $k_F |a| \ll 1$, convergence of the HFB+BMBPT3 scheme was reached for cutoffs in the range $\Lambda \lesssim 2.5 k_F$.

Given Eq. (3), which is an expansion in partial waves, it is important to investigate the number of such waves that need to be included in the calculation of the equation of state. Fig. 1 shows the HFB ground-state energy density [see Eq. (13)] in units of the energy density of the non-interacting Fermi gas (FG),

$$\mathcal{E}_{\text{FG}} = \frac{k_F^5}{10\pi^2 m} \quad (29)$$

as a function of $k_F = (3\pi^2 n)^{1/3}$, as various partial waves are included one by one, for a density dependent cutoff $\Lambda = 2 k_F$. We see that the S -wave dominates until $k_F \sim 0.4 \text{ fm}^{-1}$, beyond which the P and D waves become important. Because of strong cancellations between the 3P_0 , 3P_1 and 3P_2 contributions, including the P wave without the D wave does not result in a noticeable improvement at any density. Partial waves beyond $l = 2$ have some effect for $k_F \gtrsim 0.7 \text{ fm}^{-1}$. We conclude that for the density range we are interested in, including partial waves with $l \leq 6$ yields converged (with respect to l_{max}) results.

Let us now come back to the discussion of constant vs. density dependent cutoffs. In Fig. 2, we compare HF

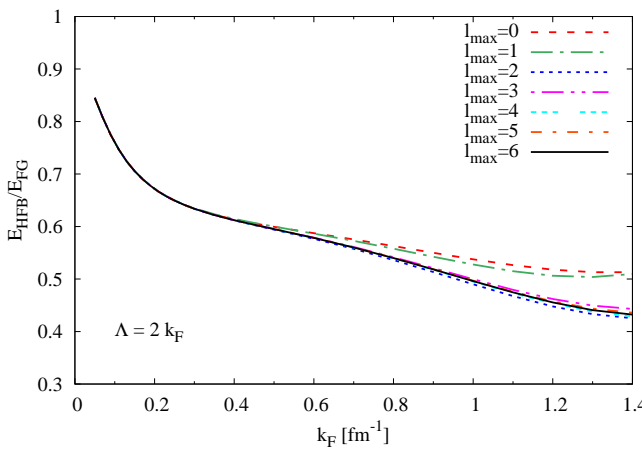


FIG. 1. Convergence of the equation of state (energy density in units of the energy density of the ideal Fermi gas as a function of k_F) in the HFB approximation with the inclusion of the higher partial waves. Here, l_{\max} indicates the highest partial wave that has been included.

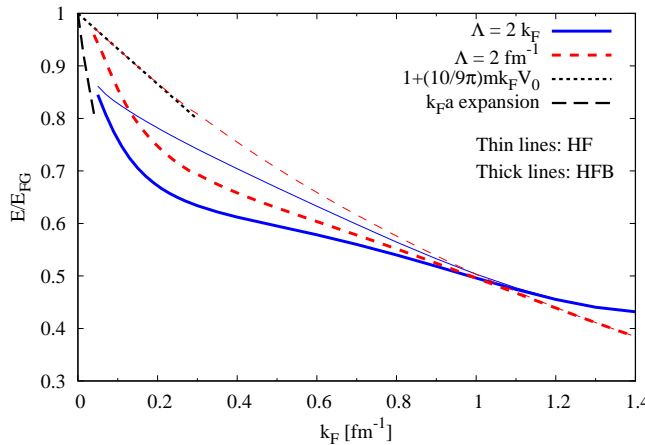


FIG. 2. HF (thin lines) and HFB (thick lines) results for the ground-state energy obtained with a fixed cutoff $\Lambda = 2 \text{ fm}^{-1}$ (red dashes) and with a density-dependent cutoff $\Lambda = 2k_F$ (blue solid lines). The short black dashes show the asymptotic low-density behavior of the HF result with fixed cutoff according to Eq. (30), while the long black dashes show the fourth-order $k_F a$ expansion of Ref. [31].

(thin lines) and HFB (thick lines) results obtained with fixed ($\Lambda = 2 \text{ fm}^{-1}$, red dashes) and density dependent ($\Lambda = 2k_F$, blue solid lines) cutoffs. It is evident that results for the constant and the density dependent cutoffs agree at $k_F = 1 \text{ fm}^{-1}$. For larger k_F , the density dependent cutoff is bigger than the fixed cutoff, reaching eventually a value of 2.8 fm^{-1} (since the figure covers the range $k_F \leq 1.4 \text{ fm}^{-1}$). We observe that at $k_F \gtrsim 1.1 \text{ fm}^{-1}$, the HFB results are practically identical to the respective HF results because the pairing gap becomes very small compared to the Fermi energy.

As the density tends towards zero, the ground state

energy of the interacting system approaches that of the non-interacting system. In HF approximation, for a fixed cutoff, one can obtain an expansion in k_F ,

$$\frac{E_{\text{HF}}}{E_{\text{FG}}} = 1 + \frac{10}{9\pi} m k_F V_0, \quad (30)$$

where $V_0 = V_{1S_0}(0,0)$ is the matrix element of the two-body interaction for $q = q' = 0$. This result, shown as black short-dashed line in Fig. 2 is in perfect agreement with the HF result (thin red dashes) up to $k_F \sim 0.2 \text{ fm}^{-1}$. The inclusion of pairing in HFB does not change this asymptotic behavior since the pairing gap vanishes as $k_F^2 e^{-\pi/|2k_F a|}$ [17], and this explains why also the HFB results (thick red dashes) eventually approach the curve given by Eq. (30) at very small k_F .

Obviously, Eq. (30) is in disagreement with the well-known leading term of the $k_F a$ expansion [27] which is given by Eq. (30) with the replacement $V_0 \rightarrow a/m$. In the case of neutron matter and $\Lambda = 2 \text{ fm}^{-1}$, the factor a/m is about ten times larger in magnitude than V_0 . Hence, the slope of the HF (and HFB) results at small k_F with fixed $\Lambda = 2 \text{ fm}^{-1}$ is much too small, as can be seen by comparing them with the results of the $k_F a$ expansion of Ref. [31] [black dashes, including orders up to $(k_F a)^4$]. Notice that the validity of this expansion is limited to the small region $k_F \lesssim 1/|a| \sim 0.05 \text{ fm}^{-1}$. Furthermore, it does not include effects of the finite range of the nn interaction.

It is well known that with decreasing cutoff, V_0 grows in magnitude until it finally approaches a/m (see, e.g., Fig. 15 in Ref. [23]). The HF(B) energies obtained with the density dependent cutoff (solid blue lines in Fig. 2) are therefore much lower (at low densities) than those obtained with the fixed cutoff, and they are in much better agreement with the $k_F a$ expansion. We conclude that, in order to reproduce the correct low-density behavior, the HFB approximation with a density dependent cutoff is a better starting point than with a fixed cutoff.

The HFB 1S_0 gap Δ_{k_F} as function of k_F , computed using Eqs. (5) and (8)-(12) for different values of the cutoff parameter $f = \Lambda/k_F$, is seen in Fig. 3(a), while Fig. 3(b) shows the corresponding effective mass, defined by

$$\frac{1}{m^*} = \frac{1}{m} + \frac{1}{k_F} \frac{d\Sigma_{\text{HFB}}(k)}{dk} \Big|_{k=k_F}. \quad (31)$$

The unusual fact that $m^* > m$ at very low density, especially for $\Lambda = 1.5 k_F$, can be understood from the shape of the matrix elements of $V_{\text{low-}k}$ in the case of very small cutoffs, see, e.g., Fig. 11 of Ref. [25]. Since the effective mass determines the density of states at the Fermi level, the gap usually reacts very sensitively to its change, a reduction of m^* leading to a reduction of the gap. But in Fig. 3 we note that, while the effective mass decreases with increasing cutoff parameter, the dependence of the gap on this parameter shows the opposite trend. The explanation is that if the cutoff gets very small ($\Lambda = 1.5 k_F$), the matrix elements of the potential and hence the gap

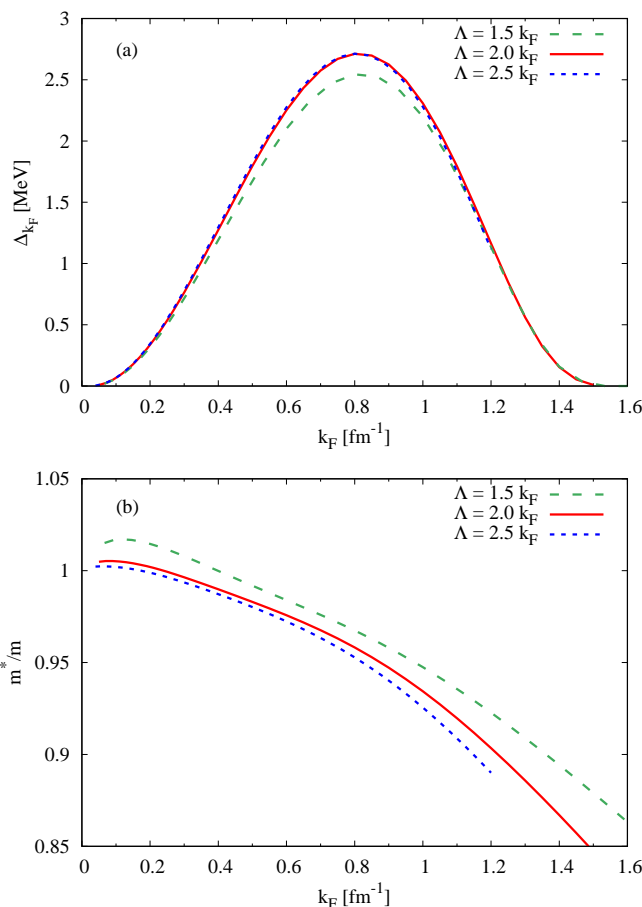


FIG. 3. (a) HFB $1S_0$ pairing gap and (b) effective mass as a function of k_F for three different values of the cutoff parameter $f = \Lambda/k_F$.

function Δ_k and the v_k factors are cut off closely above k_F so that the gap must be reduced, even though the effective mass is enhanced. For Λ/k_F between 2 and 2.5, these two effects compensate each other (the almost exact cancellation being accidental), and the gap remains practically unchanged in spite of the further reduced effective mass.

B. HFB+BMBPT results

So far, we have only discussed HFB results and their dependence on the unphysical cutoff parameter. Let us now discuss how the situation improves when we include the BMBPT corrections. In Fig. 4, we present our calculation of the equation of state within HFB+BMBPT up to third order for both fixed cutoff [$\Lambda = 2 \text{ fm}^{-1}$, Fig. 4(a)] and density dependent cutoff [$\Lambda = 2k_F$, Fig. 4(b)] as a function of k_F . In addition, we also include the HF+MBPT results obtained by setting $\Delta = 0$.

The BMBPT3 results obtained with fixed and density dependent cutoffs differ noticeably from each other

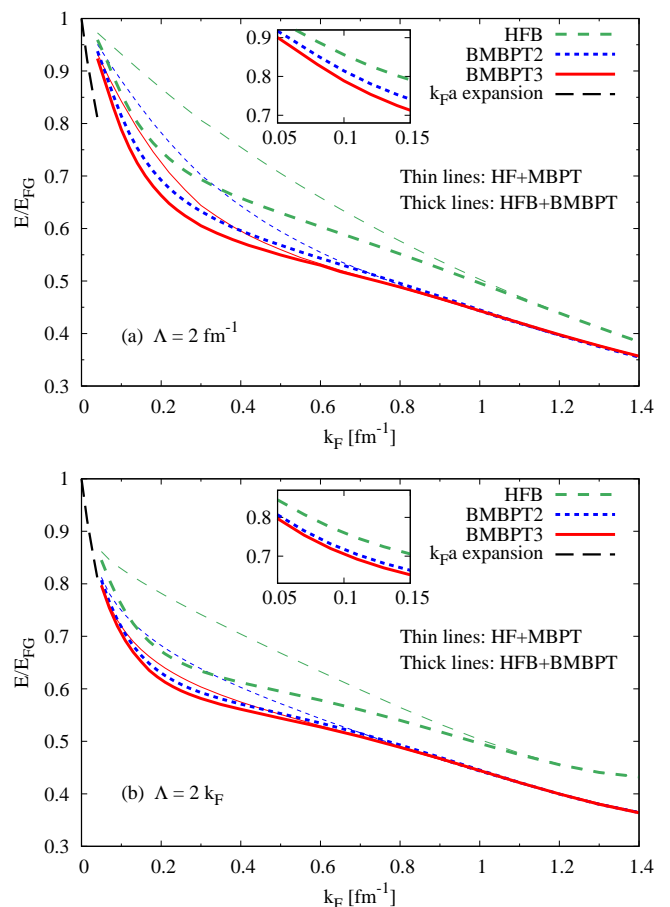


FIG. 4. Ground state energy in units of the energy of the free Fermi gas, as a function of k_F , at different levels of approximation: HFB (green dashes), BMBPT2 (short blue dashes), BMBPT3 (red solid lines), for (a) fixed cutoff $\Lambda = 2 \text{ fm}^{-1}$ and (b) density dependent cutoff $\Lambda = 2k_F$. HF and MBPT results are shown using thin lines.

in the region $k_F \lesssim 0.4 \text{ fm}^{-1}$. In particular, the energies obtained with a fixed cutoff (Fig. 4(a)) are much higher than those of the k_Fa expansion. Furthermore, the BMBPT3 correction, e.g., at $k_F = 0.1 \text{ fm}^{-1}$, is about 60 % of the BMBPT2 correction (see inset in Fig. 4(a)), so one cannot claim that the expansion has converged, and it is not clear whether perturbation theory will ever be able to bring the results down to the k_Fa expansion. On the contrary, with the density dependent cutoff (Fig. 4(b)) the agreement between BMBPT3 and k_Fa expansion is very good, and the BMBPT3 brings only a tiny correction to the BMBPT2 result, so that one may speak of convergence of the BMBPT expansion.

Let us explain these findings. At very low density, the results should agree with the k_Fa -expansion because the particles scatter at very low energies and Pauli-blocking effects are negligible. As already pointed out in the preceding subsection, in order to obtain the scattering length, one either has to resum ladders to all orders or take the limit $\Lambda \rightarrow 0$ in which case the value of

$V_0 = V_{1S_0}(0,0)$ approaches the scattering length. Hence the HFB energy with a fixed cutoff is far too high, as already seen in Fig. 2, and the third-order perturbation theory is not enough to correct for that,² whereas for density dependent cutoff, at very low k_F (and hence very low Λ), the perturbative corrections bring the results into agreement with the $k_F a$ -expansion.

At very low and high densities, the gaps become very small and HFB+BMBPT reduces in practice to the simpler HF+MBPT, plotted with thin lines. For $k_F \lesssim 1 \text{ fm}^{-1}$, where the gap is large enough to make a noticeable contribution to the equation of state, we see that the perturbative corrections within BMBPT to HFB are much lesser than those of MBPT to HF. Hence the HFB+BMBPT converges better than the HF+MBPT as expected. However, it is interesting that in the region $k_F \sim 0.6 - 1 \text{ fm}^{-1}$, both MBPT3 and BMBPT3 give practically the same results, i.e., the MBPT is able to account for the pairing correlations which are missing in the HF ground state. For $k_F \lesssim 0.6 \text{ fm}^{-1}$, the MBPT cannot reproduce the BMBPT results, at least not yet at 3rd order.

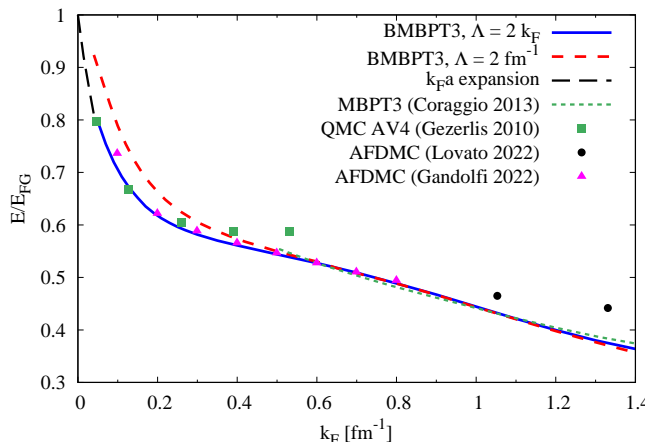


FIG. 5. BMBPT3 equation of state for fixed cutoff $\Lambda = 2 \text{ fm}^{-1}$ (red dashes) and density dependent cutoff $\Lambda = 2 k_F$ (blue solid lines). For comparison, we also show the low-density behavior according to the fourth-order $k_F a$ expansion of Ref. [31] (black long dashes), MBPT3 results of Ref. [26] (green small dashes), and various QMC results of Refs. [33] (green squares), [34] (purple triangles), and [35] (black circles).

In Fig. 5, we compare our final results (BMBPT3) with results from the literature such as MBPT [26] and

Quantum Monte Carlo (QMC) [33–35]. At low densities, our results for $\Lambda = 2 k_F$ are in excellent agreement with the QMC results [33, 34] [except the last two points of Ref. [33] (green squares) at $k_F \sim 0.4 - 0.5 \text{ fm}^{-1}$]. Furthermore, our results are also very similar to the MBPT results of Ref. [26] (green small dashes), although another interaction (chiral N3LO with $\Lambda = 500 \text{ MeV}$, no three-body force) was used there.

Looking at the region $k_F > 1 \text{ fm}^{-1}$, we have seen in Fig. 2 that the HFB results (which are close to the HF results in that region) obtained with $\Lambda = 2 \text{ fm}^{-1}$ differ from those obtained with $\Lambda = 2 k_F$. But now we see in Fig. 5 that this difference is to a large extent absorbed by the BMBPT corrections, as it should be since physical results should be cutoff independent. But we also observe that our results lie clearly below the QMC points of Ref. [35] (black circles). This difference could be due to the missing three-body force in our calculation.

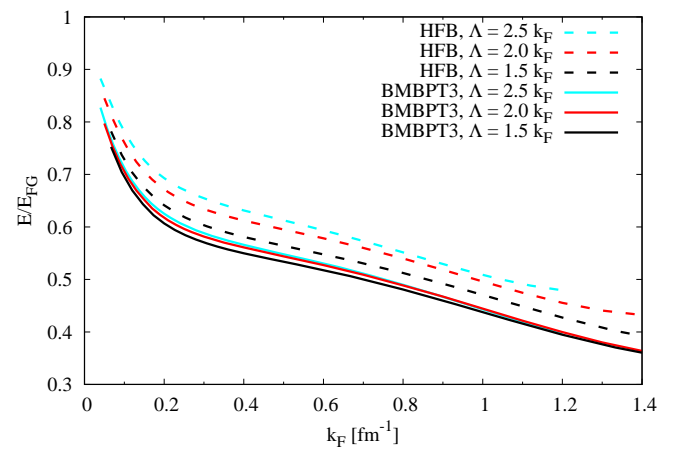


FIG. 6. HFB (dashed lines) and BMBPT3 (solid lines) equations of state for three different scale factors $f = \Lambda/k_F = 1.5$ (black), 2 (red), and 2.5 (light blue).

In Fig. 6, we study more systematically the cutoff dependence of the HFB (dashed lines) and BMBPT3 (solid lines) results by using different scale parameters $f = \Lambda/k_F$ (as in Fig. 3). Again, we note that, compared to the HFB results, the cutoff dependence is significantly reduced by including perturbative corrections up to third order. But the equation state including the third-order corrections still does have residual cutoff dependence. This could be due to missing higher-order perturbative contributions, or missing contributions of three-body forces, as discussed in the following section.

IV. SUMMARY AND OUTLOOK

In this work, we focus on calculating the equation of state for pure neutron matter with renormalization-group softened $V_{\text{low-}k}$ interactions within BMBPT that builds perturbative corrections around the HFB state and hence

² This can also be understood by looking at the so-called Weinberg eigenvalues as shown in Fig. 1 of Ref. [32]: although $\Lambda = 2 \text{ fm}^{-1}$ is enough to make the interaction soft, in the sense that all repulsive eigenvalues are small, the attractive eigenvalue becomes large at low density and hence very high orders in perturbation theory would be needed to describe the full (in-medium) T matrix.

takes into account the superfluid nature of the ground state. While pairing almost does not affect the equation of state at high densities, including it certainly gives a better starting point for the perturbation theory in the range of densities where the gap is large and where the HFB energy is considerably lower than the HF one. Furthermore, at very low densities, the HFB provides a better starting point of the perturbative expansion if one uses in the $V_{\text{low-}k}$ interaction a density dependent cutoff Λ that scales with k_F instead of a fixed cutoff.

Since the cutoff Λ is an unphysical quantity, observables such as the ground-state energy should not depend on it. While the BMBPT corrections absorb the cutoff dependence of the HFB results to a large extent, we note that there is still residual cutoff dependence after including third order. For a cutoff of $\Lambda = 2 \text{ fm}^{-1}$, the three-body forces contribute at leading order only for $k_F > 0.8 \text{ fm}^{-1}$ [36]. However, for a density dependent cutoff that scales with k_F , three- (and maybe even higher-) body forces could also play a significant role at smaller densities because then the cutoff becomes very small and the three- (and higher-) body terms may grow as the two-body term is evolved via the RG flow [23, 37]. At the very least, it would be necessary to include the induced three-body effects. An interesting approach to include the induced forces is the in-medium SRG (IM-SRG) technique that has been very successful in finite nuclei (see for example [38]). However, this is beyond the scope of our current work and will be postponed to a future study.

Furthermore, there is also a lot of interest in the superfluid properties of neutron matter, independently of the equation of state. Like the HFB ground-state energy, also the pairing gap shows dependence on the unphysical cutoff parameter Λ of the $V_{\text{low-}k}$ interaction. One may hope that, by computing higher-order perturbative corrections to the normal and anomalous self-energies (i.e., diagonal and non-diagonal in Nambu-Gor'kov indices [39]), one can obtain more cutoff independent results for the quasiparticle dispersion relation (mean field, effective mass) and for the gap. Higher-order contributions to the anomalous self-energy include, e.g., screening corrections to the gap, which are known to reduce the gap. Work in this direction is in progress.

ACKNOWLEDGMENTS

We thank L. Coraggio for sending us the data of Ref. [26]. We acknowledge support from the Collaborative Research Program of IFCPAR/CEFIPRA, Project number: 6304-4.

APPENDIX: EXPLICIT EXPRESSIONS FOR THE THIRD-ORDER BMBPT CORRECTION

For completeness, we give here the expressions necessary to compute $\Omega^{(3)}$, Eq. (27), generalizing the expressions given in the appendix of Ref. [18] to the case of non-separable interactions with partial waves beyond the 1S_0 .

Momentum conservation in \hat{K}_{04} and \hat{K}_{40} requires $\mathbf{k}_1 + \mathbf{k}_2 + \mathbf{k}_3 + \mathbf{k}_4 = 0$ and $\mathbf{k}_5 + \mathbf{k}_6 + \mathbf{k}_7 + \mathbf{k}_8 = 0$. Furthermore, \hat{K}_{22} leaves two momenta and two spins unchanged. So, there are only four independent momenta to integrate and six spins to sum over. After relabeling the particles such that the four integration variables are called $\mathbf{k}_1 \dots \mathbf{k}_4$, we can write

$$\begin{aligned} \Omega_0^{(3)} = & \sum_{\mathbf{k}_1 \dots \mathbf{k}_4} \left(u_1 v_1 u_2 v_2 u_3 v_3 u_4 v_4 A_1 \right. \\ & + u_1 v_1 u_2 v_2 u_3 v_3 v_4^2 A_2 + u_1 v_1 u_2 v_2 u_3 v_3 u_4^2 A_3 \\ & + u_1 v_1 u_2 v_2 v_3^2 v_4^2 A_4 + u_1 v_1 u_2 v_2 v_3^2 u_4^2 A_5 \\ & \left. + v_1^2 v_2^2 v_3^2 u_4^2 A_6 + v_1^2 v_2^2 u_3^2 u_4^2 A_7 \right). \end{aligned} \quad (32)$$

The remaining momenta are then given by different linear combinations of $\mathbf{k}_1 \dots \mathbf{k}_4$ which we denote by

$$\begin{aligned} \mathbf{k}_5 &= -\mathbf{k}_1 - \mathbf{k}_2 - \mathbf{k}_3, & \mathbf{k}_6 &= -\mathbf{k}_1 - \mathbf{k}_2 - \mathbf{k}_4, \\ \mathbf{k}_7 &= -\mathbf{k}_1 - \mathbf{k}_3 - \mathbf{k}_4, & \mathbf{k}_8 &= -\mathbf{k}_2 - \mathbf{k}_3 - \mathbf{k}_4, \\ \mathbf{k}_9 &= \mathbf{k}_1 + \mathbf{k}_2 - \mathbf{k}_3, & \mathbf{k}_{10} &= \mathbf{k}_1 + \mathbf{k}_3 - \mathbf{k}_2, \\ \mathbf{k}_{11} &= \mathbf{k}_1 + \mathbf{k}_2 - \mathbf{k}_4, & \mathbf{k}_{12} &= \mathbf{k}_1 + \mathbf{k}_4 - \mathbf{k}_2, \\ \mathbf{k}_{13} &= \mathbf{k}_2 + \mathbf{k}_3 - \mathbf{k}_4. \end{aligned} \quad (33)$$

Using notations

$$\begin{aligned} \langle \mathbf{k}_1 \sigma_1 \mathbf{k}_2 \sigma_2 | \bar{V} | \mathbf{k}_3 \sigma_3 \mathbf{k}_4 \sigma_4 \rangle &= \bar{V}_{\sigma_1 \sigma_2 \sigma_3 \sigma_4}(\mathbf{q}_{1,2}, \mathbf{q}_{3,4}) \\ \mathbf{q}_{i,j} &= \frac{\mathbf{k}_i - \mathbf{k}_j}{2} \quad \mathbf{q}_{i,j}^+ = \frac{\mathbf{k}_i + \mathbf{k}_j}{2}, \quad \bar{\sigma}_i = -\sigma_i, \end{aligned}$$

the expressions for the integrands $A_1 \dots A_7$ in Eq. (32) read:

$$\begin{aligned}
A_1 = & \sum_{\sigma_1 \dots \sigma_6} \left[(-1)^{\sigma_3 + \sigma_6} u_5^2 u_6^2 \frac{\text{Re} [\bar{V}_{\sigma_2 \sigma_4 \bar{\sigma}_6 \bar{\sigma}_1}(\mathbf{q}_{2,4}, \mathbf{q}_{1,6}) \bar{V}_{\bar{\sigma}_3 \bar{\sigma}_1 \sigma_2 \sigma_5}(\mathbf{q}_{1,3}, \mathbf{q}_{2,5}) \bar{V}_{\sigma_3 \sigma_5 \sigma_4 \sigma_6}(\mathbf{q}_{3,5}, \mathbf{q}_{4,6})]}{E_{1,2,3,5} E_{1,2,4,6}} \right. \\
& + (-1)^{\sigma_3 + \sigma_6} v_5^2 v_6^2 \frac{\text{Re} [\bar{V}_{\sigma_1 \sigma_4 \bar{\sigma}_6 \bar{\sigma}_2}(\mathbf{q}_{1,4}, \mathbf{q}_{2,6}) \bar{V}_{\bar{\sigma}_3 \bar{\sigma}_2 \sigma_1 \sigma_5}(\mathbf{q}_{2,3}, \mathbf{q}_{1,5}) \bar{V}_{\sigma_3 \sigma_5 \sigma_4 \sigma_6}(\mathbf{q}_{3,5}, \mathbf{q}_{4,6})]}{E_{1,2,3,5} E_{1,2,4,6}} \\
& - (-1)^{\sigma_2 + \sigma_3 + \sigma_5 + \sigma_6} (u_5^2 u_{13}^2 + v_5^2 v_{13}^2) \frac{\text{Re} [\bar{V}_{\sigma_1 \sigma_4 \bar{\sigma}_5 \bar{\sigma}_6}(\mathbf{q}_{1,4}, \mathbf{q}_{13,5}) \bar{V}_{\sigma_2 \sigma_3 \sigma_6 \sigma_4}(\mathbf{q}_{2,3}, \mathbf{q}_{13,4}) \bar{V}_{\bar{\sigma}_3 \bar{\sigma}_2 \sigma_1 \sigma_5}(\mathbf{q}_{2,3}, \mathbf{q}_{1,5})]}{E_{1,4,5,13} E_{1,2,3,5}} \\
& - (-1)^{\sigma_3 + \sigma_5} u_5 v_5 u_6 v_6 \frac{\text{Re} [\bar{V}_{\sigma_2 \sigma_4 \bar{\sigma}_6 \bar{\sigma}_1}(\mathbf{q}_{2,4}, \mathbf{q}_{1,6}) \bar{V}_{\bar{\sigma}_3 \bar{\sigma}_1 \sigma_2 \sigma_5}(\mathbf{q}_{1,3}, \mathbf{q}_{2,5}) \bar{V}_{\sigma_3 \bar{\sigma}_6 \sigma_4 \bar{\sigma}_5}(\mathbf{q}_{3,6}^+, \mathbf{q}_{4,5}^+)]}{E_{1,2,3,5} E_{1,2,4,6}} \\
& + 2 (-1)^{\sigma_1 + \sigma_6} (u_8^2 v_7^2 + u_7^2 v_8^2) \frac{\text{Re} [\bar{V}_{\sigma_1 \sigma_4 \bar{\sigma}_5 \bar{\sigma}_3}(\mathbf{q}_{1,4}, \mathbf{q}_{3,7}) \bar{V}_{\bar{\sigma}_3 \sigma_2 \sigma_4 \bar{\sigma}_6}(\mathbf{q}_{2,3}, \mathbf{q}_{4,8}) \bar{V}_{\bar{\sigma}_5 \bar{\sigma}_1 \sigma_6 \sigma_2}(\mathbf{q}_{1,7}, \mathbf{q}_{2,8})]}{E_{1,2,7,8} E_{1,3,4,7}} \\
& \left. + (-1)^{\sigma_1 + \sigma_2 + \sigma_3 + \sigma_4} u_6^2 v_5^2 \frac{\text{Re} [\bar{V}_{\sigma_1 \sigma_2 \bar{\sigma}_6 \bar{\sigma}_4}(\mathbf{q}_{1,2}, \mathbf{q}_{4,6}) \bar{V}_{\bar{\sigma}_2 \bar{\sigma}_1 \sigma_3 \sigma_5}(\mathbf{q}_{1,2}, \mathbf{q}_{3,5}) \bar{V}_{\sigma_5 \bar{\sigma}_6 \sigma_4 \bar{\sigma}_3}(\mathbf{q}_{5,6}^+, \mathbf{q}_{3,4}^+)]}{E_{1,2,3,5} E_{1,2,4,6}} \right], \quad (34)
\end{aligned}$$

$$\begin{aligned}
A_2 = & \sum_{\sigma_1 \dots \sigma_6} \left[u_6^2 u_9 v_9 \frac{\text{Re} [\bar{V}_{\sigma_2 \bar{\sigma}_5 \sigma_3 \bar{\sigma}_1}(\mathbf{q}_{2,9}, \mathbf{q}_{1,3}) \bar{V}_{\sigma_3 \sigma_6 \bar{\sigma}_5 \bar{\sigma}_4}(\mathbf{q}_{3,6}, \mathbf{q}_{4,9}) \bar{V}_{\bar{\sigma}_4 \bar{\sigma}_1 \sigma_2 \sigma_6}(\mathbf{q}_{1,4}, \mathbf{q}_{2,6})]}{E_{1,2,4,6} E_{3,4,6,9}} \right. \\
& - 2 (-1)^{\sigma_1 + \sigma_2 + \sigma_4 + \sigma_6} u_6^2 u_5 v_5 \frac{\text{Re} [\bar{V}_{\sigma_2 \sigma_3 \bar{\sigma}_5 \bar{\sigma}_1}(\mathbf{q}_{2,3}, \mathbf{q}_{1,5}) \bar{V}_{\bar{\sigma}_4 \bar{\sigma}_2 \sigma_1 \sigma_6}(\mathbf{q}_{2,4}, \mathbf{q}_{1,6}) \bar{V}_{\sigma_4 \bar{\sigma}_5 \sigma_3 \bar{\sigma}_6}(\mathbf{q}_{4,5}^+, \mathbf{q}_{3,6}^+)]}{E_{1,2,3,5} E_{1,2,4,6}} \\
& + \frac{1}{8} (-1)^{\sigma_1 + \sigma_2 + \sigma_3 + \sigma_5} u_9 v_9 v_6^2 \frac{\text{Re} [\bar{V}_{\sigma_1 \sigma_2 \sigma_3 \sigma_5}(\mathbf{q}_{1,2}, \mathbf{q}_{3,9}) \bar{V}_{\bar{\sigma}_2 \bar{\sigma}_1 \sigma_4 \sigma_6}(\mathbf{q}_{1,2}, \mathbf{q}_{4,6}) \bar{V}_{\sigma_4 \sigma_6 \bar{\sigma}_5 \bar{\sigma}_3}(\mathbf{q}_{4,6}, \mathbf{q}_{3,9})]}{E_{1,2,4,6} E_{3,4,6,9}} \\
& \left. + \frac{1}{4} (-1)^{\sigma_1 + \sigma_2 + \sigma_4 + \sigma_6} u_5 v_5 v_6^2 \frac{\text{Re} [\bar{V}_{\sigma_1 \sigma_2 \bar{\sigma}_5 \bar{\sigma}_3}(\mathbf{q}_{1,2}, \mathbf{q}_{3,5}) \bar{V}_{\bar{\sigma}_2 \bar{\sigma}_1 \sigma_4 \sigma_6}(\mathbf{q}_{1,2}, \mathbf{q}_{4,6}) \bar{V}_{\bar{\sigma}_5 \bar{\sigma}_3 \bar{\sigma}_6 \bar{\sigma}_4}(\mathbf{q}_{3,5}, \mathbf{q}_{4,6})]}{E_{1,2,3,5} E_{1,2,4,6}} \right], \quad (35)
\end{aligned}$$

$$\begin{aligned}
A_3 = & \sum_{\sigma_1 \dots \sigma_6} \left[\frac{1}{4} (-1)^{\sigma_1 + \sigma_2 + \sigma_4 + \sigma_6} u_6^2 u_5 v_5 \frac{\text{Re} [\bar{V}_{\sigma_1 \sigma_2 \bar{\sigma}_6 \bar{\sigma}_4}(\mathbf{q}_{1,2}, \mathbf{q}_{4,6}) \bar{V}_{\bar{\sigma}_2 \bar{\sigma}_1 \sigma_3 \sigma_5}(\mathbf{q}_{1,2}, \mathbf{q}_{3,5}) \bar{V}_{\sigma_3 \sigma_5 \sigma_4 \sigma_6}(\mathbf{q}_{3,5}, \mathbf{q}_{4,6})]}{E_{1,2,3,5} E_{1,2,4,6}} \right. \\
& + \frac{1}{8} (-1)^{\sigma_1 + \sigma_2 + \sigma_3 + \sigma_5} u_6^2 u_9 v_9 \frac{\text{Re} [\bar{V}_{\sigma_1 \sigma_2 \sigma_3 \sigma_5}(\mathbf{q}_{1,2}, \mathbf{q}_{3,9}) \bar{V}_{\bar{\sigma}_2 \bar{\sigma}_1 \sigma_4 \sigma_6}(\mathbf{q}_{1,2}, \mathbf{q}_{4,6}) \bar{V}_{\sigma_4 \sigma_6 \bar{\sigma}_5 \bar{\sigma}_3}(\mathbf{q}_{4,6}, \mathbf{q}_{3,9})]}{E_{1,2,4,6} E_{3,4,6,9}} \left. \right], \quad (36)
\end{aligned}$$

$$\begin{aligned}
A_4 = & \sum_{\sigma_1 \dots \sigma_6} \left[-2 (-1)^{\sigma_3 + \sigma_5} u_{13}^2 u_5^2 \frac{\text{Re} [\bar{V}_{\sigma_1 \sigma_4 \bar{\sigma}_5 \bar{\sigma}_6}(\mathbf{q}_{1,4}, \mathbf{q}_{13,5}) \bar{V}_{\bar{\sigma}_3 \bar{\sigma}_2 \sigma_1 \sigma_5}(\mathbf{q}_{2,3}, \mathbf{q}_{1,5}) \bar{V}_{\sigma_3 \bar{\sigma}_6 \sigma_4 \bar{\sigma}_2}(\mathbf{q}_{13,3}^+, \mathbf{q}_{2,4}^+)]}{E_{1,4,5,13} E_{1,2,3,5}} \right. \\
& - (-1)^{\sigma_3 + \sigma_5} u_5^2 u_6^2 \frac{\text{Re} [\bar{V}_{\sigma_2 \sigma_4 \bar{\sigma}_6 \bar{\sigma}_1}(\mathbf{q}_{2,4}, \mathbf{q}_{1,6}) \bar{V}_{\bar{\sigma}_3 \bar{\sigma}_1 \sigma_2 \sigma_5}(\mathbf{q}_{1,3}, \mathbf{q}_{2,5}) \bar{V}_{\sigma_3 \bar{\sigma}_6 \sigma_4 \bar{\sigma}_5}(\mathbf{q}_{3,6}^+, \mathbf{q}_{4,5}^+)]}{E_{1,2,3,5} E_{1,2,4,6}} \\
& - (-1)^{\sigma_2 + \sigma_3 + \sigma_4 + \sigma_6} u_7^2 v_8^2 \frac{\text{Re} [\bar{V}_{\sigma_1 \sigma_5 \bar{\sigma}_2 \bar{\sigma}_6}(\mathbf{q}_{1,8}^+, \mathbf{q}_{2,7}^+) \bar{V}_{\sigma_3 \sigma_4 \sigma_5 \sigma_2}(\mathbf{q}_{3,4}, \mathbf{q}_{2,8}) \bar{V}_{\bar{\sigma}_4 \bar{\sigma}_3 \sigma_1 \sigma_6}(\mathbf{q}_{3,4}, \mathbf{q}_{1,7})]}{E_{1,2,7,8} E_{1,3,4,7}} \\
& + 2 (-1)^{\sigma_1 + \sigma_2 + \sigma_3 + \sigma_4 + \sigma_5 + \sigma_6} u_{11}^2 u_5^2 \frac{\text{Re} [\bar{V}_{\sigma_2 \sigma_3 \bar{\sigma}_5 \bar{\sigma}_1}(\mathbf{q}_{2,3}, \mathbf{q}_{1,5}) \bar{V}_{\bar{\sigma}_4 \bar{\sigma}_3 \sigma_6 \sigma_5}(\mathbf{q}_{3,4}, \mathbf{q}_{11,5}) \bar{V}_{\sigma_4 \bar{\sigma}_2 \sigma_1 \bar{\sigma}_6}(\mathbf{q}_{2,4}^+, \mathbf{q}_{1,11}^+)]}{E_{1,2,3,5} E_{3,4,5,11}} \\
& - \frac{1}{2} (-1)^{\sigma_1 + \sigma_3 + \sigma_4 + \sigma_6} u_7^2 u_8^2 \frac{\text{Re} [\bar{V}_{\sigma_3 \sigma_4 \bar{\sigma}_6 \bar{\sigma}_2}(\mathbf{q}_{3,4}, \mathbf{q}_{2,8}) \bar{V}_{\bar{\sigma}_4 \bar{\sigma}_3 \sigma_1 \sigma_5}(\mathbf{q}_{3,4}, \mathbf{q}_{1,7}) \bar{V}_{\sigma_5 \bar{\sigma}_2 \sigma_6 \bar{\sigma}_1}(\mathbf{q}_{2,7}^+, \mathbf{q}_{1,8}^+)]}{E_{1,3,4,7} E_{2,3,4,8}} \\
& + (-1)^{\sigma_1 + \sigma_3 + \sigma_5 + \sigma_6} u_7^2 v_{12}^2 \frac{\text{Re} [\bar{V}_{\bar{\sigma}_2 \bar{\sigma}_5 \bar{\sigma}_4 \bar{\sigma}_1}(\mathbf{q}_{12,2}, \mathbf{q}_{1,4}) \bar{V}_{\sigma_4 \bar{\sigma}_3 \sigma_1 \sigma_6}(\mathbf{q}_{3,4}, \mathbf{q}_{1,7}) \bar{V}_{\sigma_5 \bar{\sigma}_3 \bar{\sigma}_6 \bar{\sigma}_2}(\mathbf{q}_{12,3}, \mathbf{q}_{2,7})]}{E_{1,3,4,7} E_{2,3,7,12}} \\
& \left. - 2 (-1)^{\sigma_2 + \sigma_3 + \sigma_4 + \sigma_6} u_5^2 u_7^2 \frac{\text{Re} [\bar{V}_{\bar{\sigma}_3 \bar{\sigma}_1 \sigma_2 \sigma_5}(\mathbf{q}_{1,3}, \mathbf{q}_{2,5}) \bar{V}_{\sigma_3 \sigma_4 \bar{\sigma}_6 \bar{\sigma}_1}(\mathbf{q}_{3,4}, \mathbf{q}_{1,7}) \bar{V}_{\sigma_5 \bar{\sigma}_4 \sigma_6 \bar{\sigma}_2}(\mathbf{q}_{4,5}^+, \mathbf{q}_{2,7}^+)]}{E_{1,2,3,5} E_{1,3,4,7}} \right], \quad (37)
\end{aligned}$$

$$\begin{aligned}
A_5 = & \sum_{\sigma_1 \dots \sigma_6} \left[(-1)^{\sigma_1 + \sigma_3 + \sigma_4 + \sigma_6} u_7^2 u_8^2 \frac{\text{Re} [\bar{V}_{\sigma_1 \sigma_5 \sigma_2 \sigma_6}(\mathbf{q}_{1,7}, \mathbf{q}_{2,8}) \bar{V}_{\sigma_2 \sigma_3 \bar{\sigma}_6 \bar{\sigma}_4}(\mathbf{q}_{2,3}, \mathbf{q}_{4,8}) \bar{V}_{\bar{\sigma}_3 \bar{\sigma}_1 \sigma_4 \sigma_5}(\mathbf{q}_{1,3}, \mathbf{q}_{4,7})]}{E_{1,3,4,7} E_{2,3,4,8}} \right. \\
& + \frac{1}{2} (-1)^{\sigma_1 + \sigma_4 + \sigma_5 + \sigma_6} u_7^2 v_{10}^2 \frac{\text{Re} [\bar{V}_{\sigma_1 \bar{\sigma}_5 \sigma_2 \bar{\sigma}_3}(\mathbf{q}_{1,10}^+, \mathbf{q}_{2,3}^+) \bar{V}_{\bar{\sigma}_3 \bar{\sigma}_1 \sigma_4 \sigma_6}(\mathbf{q}_{1,3}, \mathbf{q}_{4,7}) \bar{V}_{\sigma_5 \sigma_2 \bar{\sigma}_6 \bar{\sigma}_4}(\mathbf{q}_{10,2}, \mathbf{q}_{4,7})]}{E_{1,3,4,7} E_{2,4,7,10}} \\
& \left. - (-1)^{\sigma_2 + \sigma_3 + \sigma_4 + \sigma_5} u_5^2 u_7^2 \frac{\text{Re} [\bar{V}_{\sigma_2 \sigma_3 \bar{\sigma}_6 \bar{\sigma}_1}(\mathbf{q}_{2,3}, \mathbf{q}_{1,5}) \bar{V}_{\bar{\sigma}_3 \bar{\sigma}_1 \sigma_4 \sigma_5}(\mathbf{q}_{1,3}, \mathbf{q}_{4,7}) \bar{V}_{\bar{\sigma}_6 \bar{\sigma}_2 \bar{\sigma}_5 \bar{\sigma}_4}(\mathbf{q}_{2,5}, \mathbf{q}_{4,7})]}{E_{1,2,3,5} E_{1,3,4,7}} \right], \quad (38)
\end{aligned}$$

$$\begin{aligned}
A_6 = & \sum_{\sigma_1 \dots \sigma_6} \left[- (-1)^{\sigma_1 + \sigma_2 + \sigma_4 + \sigma_5} u_6^2 u_7^2 \frac{\text{Re} [\bar{V}_{\sigma_1 \sigma_3 \bar{\sigma}_6 \bar{\sigma}_4}(\mathbf{q}_{1,3}, \mathbf{q}_{4,7}) \bar{V}_{\bar{\sigma}_2 \bar{\sigma}_1 \sigma_4 \sigma_5}(\mathbf{q}_{1,2}, \mathbf{q}_{4,6}) \bar{V}_{\sigma_2 \bar{\sigma}_6 \sigma_3 \bar{\sigma}_5}(\mathbf{q}_{2,7}^+, \mathbf{q}_{3,6}^+)]}{E_{1,2,4,6} E_{1,3,4,7}} \right. \\
& + \frac{1}{8} (-1)^{\sigma_1 + \sigma_2 + \sigma_3 + \sigma_5} u_6^2 v_9^2 \frac{\text{Re} [\bar{V}_{\sigma_1 \sigma_2 \sigma_3 \sigma_5}(\mathbf{q}_{12}, \mathbf{q}_{39}) \bar{V}_{\bar{\sigma}_2 \bar{\sigma}_1 \sigma_4 \sigma_6}(\mathbf{q}_{1,2}, \mathbf{q}_{4,6}) \bar{V}_{\sigma_4 \sigma_6 \bar{\sigma}_5 \bar{\sigma}_3}(\mathbf{q}_{4,6}, \mathbf{q}_{3,9})]}{E_{1,2,4,6} E_{3,4,6,9}} \left. \right] \quad (39)
\end{aligned}$$

$$A_7 = \sum_{\sigma_1 \dots \sigma_6} \frac{1}{8} (-1)^{\sigma_1 + \sigma_2 + \sigma_4 + \sigma_6} u_5^2 u_6^2 \frac{\text{Re} [\bar{V}_{\sigma_1 \sigma_2 \bar{\sigma}_6 \bar{\sigma}_4}(\mathbf{q}_{1,2}, \mathbf{q}_{4,6}) \bar{V}_{\bar{\sigma}_2 \bar{\sigma}_1 \sigma_3 \sigma_5}(\mathbf{q}_{1,2}, \mathbf{q}_{3,5}) \bar{V}_{\sigma_3 \sigma_5 \sigma_4 \sigma_6}(\mathbf{q}_{3,5}, \mathbf{q}_{4,6})]}{E_{1,2,3,5} E_{1,2,4,6}}. \quad (40)$$

[1] N. Chamel and P. Haensel, Living Rev. Rel. **11** (2008), 10 [doi:10.12942/lrr-2008-10].

[2] P. W. Anderson and N. Itoh, Nature (London) **256**, 25 (1975).

[3] N. Chamel, Phys. Rev. C **85**, 035801 (2012).

[4] N. Andersson, K. Glampedakis, W. C. G. Ho, and C. M. Espinoza, Phys. Rev. Lett. **109**, 241103 (2012).

[5] N. Martin and M. Urban, Phys. Rev. C **94**, 065801 (2016).

[6] G. Włazłowski, K. Sekizawa, P. Magierski, A. Bulgac, and M. M. Forbes, Phys. Rev. Lett. **117**, 232701 (2016).

[7] D. G. Yakovlev and C. J. Pethick, Ann. Rev. Astron. Astrophys. **42**, 169 (2004).

[8] A. B. Migdal, Zh. Eksp. Teor. Fiz. **37**, 249 (1959).

[9] N. Martin and M. Urban, Phys. Rev. C **92**, 015803 (2015).

[10] S. Ramanan and M. Urban, Eur. Phys. J. ST **230**, 567 (2021).

[11] J. M. Dong, U. Lombardo and W. Zuo, Phys. Rev. C **87**, 062801(R) (2013).

[12] S. Maurizio, J. W. Holt, and P. Finelli, Phys. Rev. C **90**, 044003 (2014).

[13] S. Srinivas and S. Ramanan, Phys. Rev. C **94**, 064303 (2016).

[14] C. Drischler, T. Krüger, K. Hebeler and A. Schwenk, Phys. Rev. C **95**, 024302 (2017).

[15] P. Papakonstantinou and J. W. Clark, J. Low Temp. Phys. **189**, 361 (2017).

[16] G. A. Baker, Phys. Rev. C **60**, 054311 (1999).

[17] G. Calvanese Strinati, P. Pieri, G. Röpke, P. Schuck, and M. Urban, Phys. Rep. **738**, 1 (2018).

[18] M. Urban and S. Ramanan, Phys. Rev. A **103**, 063306 (2021).

[19] A. Tichai, P. Arthuis, T. Duguet, H. Hergert, V. Somà, and R. Roth, Phys. Lett. B **786**, 195 (2018).

[20] S. Bogner, T. T. S. Kuo, L. Coraggio, A. Covello, and N. Itaco, Phys. Rev. C **65**, 051301(R) (2002).

[21] S. Bogner, T. T. S. Kuo and A. Schwenk, Phys. Rep. **386**, 1 (2003).

[22] S. K. Bogner, R. J. Furnstahl, S. Ramanan, and A. Schwenk, Nucl. Phys. A **784**, 79 (2007).

[23] S. K. Bogner, R. J. Furnstahl and A. Schwenk, Prog. Part. Nucl. Phys. **65** 94, (2010).

[24] A. Schwenk, B. Friman and G. E. Brown, Nucl. Phys. A **713**, 191 (2003).

[25] S. Ramanan and M. Urban, Phys. Rev. C **98**, 024314 (2018).

[26] L. Coraggio, J. W. Holt, N. Itaco, R. Machleidt and F. Sammarruca, Phys. Rev. C **87**, 014322 (2013).

[27] A. L. Fetter and J. D. Walecka, *Quantum Theory of Many-Particle Systems* (McGraw-Hill, New York, 1971).

[28] D. A. Varshalovich, A. N. Moskalev, and V. K. Kerhonskii, *Quantum Theory of Angular Momentum* (World Scientific, Singapore, 1988).

[29] R. B. Wiringa, V. G. J. Stoks, and R. Schiavilla, Phys. Rev. C **51**, 38 (1995).

[30] D. R. Entem and R. Machleidt, Phys. Rev. C **68**, 041001(R) (2003).

[31] C. Wellenhofer, C. Drischler, and A. Schwenk, Phys. Rev. C **104**, 014003 (2021).

[32] S. Ramanan, S. K. Bogner and R. J. Furnstahl, Nucl. Phys. A **797**, 81 (2007).

[33] A. Gezerlis and J. Carlson, Phys. Rev. C **81**, 025803 (2010).

[34] S. Gandolfi, G. Palkanoglou, J. Carlson, A. Gezerlis and K. E. Schmidt, Condens. Mat. **7**, 19 (2022).

- [35] A. Lovato, I. Bombaci, D. Logoteta, M. Piarulli and R. B. Wiringa, Phys. Rev. C **105**, 055808 (2022).
- [36] K. Hebel and A. Schwenk, Phys. Rev. C **82**, 014314 (2010).
- [37] A. Nogga, S. K. Bogner, and A. Schwenk, Phys. Rev. C **70**, 061002(R) (2004).
- [38] H. Hergert, S. K. Bogner, T. D. Morris, A. Schwenk and K. Tsukiyama, Phys. Rep. **621** 165, (2016).
- [39] J. R. Schrieffer, *Theory of Superconductivity* (Benjamin, New York, 1964).